Salud, Ciencia y Tecnología - Serie de Conferencias. 2024; 3:936
doi: 10.56294/sctconf2024936

Category: STEM (Science, Technology, Engineering and Mathematics)

ORIGINAL

Advancements in Image Enhancement and Attention based EfficientDet Optimization Classifier for Precise Osteosarcoma Lung Nodule Detection

Avances en la Mejora de Imágenes y el Clasificador de Optimización EfficientDet basado en la Atención para la Detección Precisa de Nódulos Pulmonares de Osteosarcoma

Nandhini. A[1], Sengaliappan. M[1]

[1]Department of Computer Applications, Nehru College of Management. Coimbatore.

Cite as: Nandhini. A, Sengaliappan M. Advancements in Image Enhancement and Attention based EfficientDet Optimization Classifier for Precise Osteosarcoma Lung Nodule Detection. Salud, Ciencia y Tecnología - Serie de Conferencias. 2024; 3:936. https://doi.org/10.56294/sctconf2024936

Submitted: 10-02-2024 **Revised:** 03-05-2024 **Accepted:** 20-06-2024 **Published:** 21-06-2024

Editor: Dr. William Castillo-González

ABSTRACT

Introduction: osteosarcoma is a malignant bone tumor that frequently spreads to the lungs, hence therapy effectiveness depends on early identification. However, noise and subtle characteristics still pose a challenge for reliable Lung Nodules Detection (LND) in medical pictures. In earlier work, SSD-VGG16 was implemented to provide a bounding box with an accuracy score that represented a single osteosarcoma nodule. Increasing model complexity is sometimes necessary to achieve improved accuracy with current approaches, which might worsen their computing inefficiencies.
Method: for accurate osteosarcoma lung nodule identification, this study offers the hybrid Dynamic Virtual Bats Algorithm with Attention based Efficient Object identification (A- EfficientDet). In order to improve the quality and informativeness of clinical pictures, this study suggests including Chebyshev filtering into the pre-processing pipeline. It focuses on CT scans for the purpose of detecting lung nodules associated with osteosarcoma. Additionally, provide the optimized A-EfficientDet model, a hybrid EfficientDet model improved using the DVBA optimization technique for accurate lung nodule identification.
Results: the effectiveness of the suggested strategy in attaining accurate osteosarcoma LND is demonstrated by the experimental findings. Chebyshev filtering is incorporated during the pre-processing step, which leads to more accurate detection findings by improving the signal-to-noise ratio (SNR) and lung nodule visibility.
Conclusion: additionally, the improved EfficientDet model demonstrates its suitability for clinical applications in early osteosarcoma detection and treatment monitoring by achieving (SOTA) State-Of-The-Art execution by the metrics of sensitivity, specificity, and F1 score.

Keywords: Osteosarcoma; Lung Nodule (LN); Dynamic Virtual Bats Algorithm (DVBA); Attention Based EfficientDet; Chebyshev Filtering.

RESUMEN

Introducción: el osteosarcoma es un tumor óseo maligno que frecuentemente se disemina a los pulmones, por lo que la efectividad del tratamiento depende de su identificación temprana. Sin embargo, el ruido y las características sutiles todavía plantean un desafío para la detección confiable de nódulos pulmonares (LND) en imágenes médicas. En trabajos anteriores, se implementó SSD-VGG16 para proporcionar un cuadro delimitador con una puntuación de precisión que representaba un único nódulo de osteosarcoma. A veces es necesario aumentar la complejidad del modelo para lograr una mayor precisión con los enfoques actuales, lo que podría empeorar sus ineficiencias informáticas.

Método: para una identificación precisa de los nódulos pulmonares de osteosarcoma, este estudio ofrece el algoritmo híbrido de murciélagos virtuales dinámicos con identificación eficiente de objetos basada en la atención (A-EfficientDet). Para mejorar la calidad y el contenido informativo de los cuadros clínicos, este estudio sugiere incluir el filtrado de Chebyshev en el proceso de preprocesamiento. Se centra en las tomografías computarizadas con el fin de detectar nódulos pulmonares asociados con el osteosarcoma. Además, proporcione el modelo A-EfficientDet optimizado, un modelo híbrido EfficientDet mejorado mediante la técnica de optimización DVBA para una identificación precisa de los nódulos pulmonares.
Resultados: los hallazgos experimentales demuestran la eficacia de la estrategia sugerida para lograr una LND precisa del osteosarcoma. El filtrado de Chebyshev se incorpora durante el paso de preprocesamiento, lo que conduce a hallazgos de detección más precisos al mejorar la relación señal-ruido (SNR) y la visibilidad de los nódulos pulmonares.
Conclusión: además, el modelo EfficientDet mejorado demuestra su idoneidad para aplicaciones clínicas en la detección temprana del osteosarcoma y el seguimiento del tratamiento al lograr una ejecución de vanguardia (SOTA) mediante métricas de sensibilidad, especificidad y puntuación F1.

Palabras clave: Osteosarcoma; Nódulo Pulmonar (LN); Algoritmo Dinámico de Murciélagos Virtuales (DVBA); EfficientDet Basado en la Atención; Filtrado de Chebyshev.

INTRODUCTION

The most frequent malignant bone tumour in children as well as adolescents is osteosarcoma.The survival outcome of nonmetastatic extremity osteosarcomas has significantly increased over the years, largely due to the incorporation of multiagent chemotherapy to radical surgery.[1] Despite the advances in systemic therapy, about 30 %–40 % of extremity osteosarcoma patients relapse and >80 % of these relapses localize in the lungs.[2] Further, 20 % of the patients present with metastatic cancer during the treatment stage; the lungs is the most usual metastatic site.[3] Undoubtedly, the chosen technique for the management of respectable pulmonary metastases from extremity osteosarcomas is metastasectomy. However, due to the heterogeneity of the available evidences which is largely retrospective, a standardized protocol of management for patients with pulmonary metastases from extremity osteosarcomas has not yet fully evolved. Here expected to study the clinicopathological appearances and survival impacts of our patient cohort with pulmonary metastases from extremity osteosarcoma and additionally, briefly review the published literature.

Artificial intelligence (AI)-assisted diagnostic technology has seen a surge in use in clinical fields in the past few years. According to this research, the average accuracy rate of the NN (Neural Network) Model in 1 000 FP (fundus photographs) of diabetic patients was 93,5 %; 2 ophthalmologists identified 298 of the eyes as having DR.[4] Certain traits must be identified and assessed in order to identify malignant nodules. Cancer chance can be determined by combining the features that have been identified. Even for a skilled physician, this endeavor is exceedingly challenging because there is a challenging correlation between the presence of a nodule and a positive cancer diagnosis. Typical Computer-Aided Diagnostic (CAD) methods employ the use of previously researched characteristics, like volume, form, subtlety, solidity, spiculation, and sphericity, that are connected in some way to cancer suspicion. To identify if the nodule is benign or cancerous, they employ these traits along with Machine Learning (ML) techniques like Support Vector Machine (SVM). While many works employ comparable ML models[5,6,7,8,9,10] the drawback of these approaches is that many parameters must be hand-crafted for the framework to function at its peak, which makes it challenging to replicate SOTA outcomes. This also means that these methods are susceptible to variations in screening parameters and CT scan variations.

For endovascular treatment eligibility, a Deep Learning (DL) method produced a voxel wise area under the curve of 0,94 and a subject level accuracy of 92 %.[11] Convolutional Neural Networks (CNNs) were used in another research's method, which demonstrated the ability to effectively gather data on a mean of 92 % of clinically important coronary artery segments.[12] Thus, this research set out to determine how well the AI diagnostic DCNN framework performed in assessing pulmonary nodules in patients with osteosarcoma who were adolescents or young adults. A comparison of its clinical value against a different manual approach was a further objective of the current investigation.

Medical professionals have to work a lot of hours for evaluating lung CT images visually. AI-assisted diagnosis technology has been increasingly applied in clinical fields in the past few years. AI imaging technology can increase doctors' productivity and has a high accuracy rate, according to several research.[13] As the number of precautionary and early detection methods rises as predicted, researchers are developing automated solutions that minimize the workload of physicians, boost the accuracy of diagnostics by lowering subjectivity, expedite analysis, and lower clinical expenses.

DL has the benefit of enabling end-to-end detection in CAD programs by teaching it to recognize the most important features throughout training. As a result, the network can withstand fluctuations since it may detect

https://doi.org/10.56294/sctconf2024936

the characteristics of nodules in different CT images with different parameters.[14] Better outcomes are made possible by the framework's innate ability for invariant features learning from malignant nodules due to a training set rich in variability. Because no features are designed, the network can use the given ground-truth to independently understand the relationship among features and cancer.

This study suggests a hybrid approach that combines the DVBA with an Attention-based EfficientDet model for precise osteosarcoma lung nodule detection. The inclusion of Chebyshev filtering in the pre-processing pipeline aims for improving the quality and informativeness of clinical images, specifically focusing on CT scans for osteosarcoma lung nodule detection. For the purpose of enhancing LND accuracy, the hybrid A-EfficientDet framework optimizing with the DVBA technique. Through attaining the above optimization procedure, superior detection outcomes are achieved. As, this method is effective in generating accurate osteosarcoma LND and it is evident through the outcomes of the experiment. The pre-processing stage of the implementation of Chebyshev filtering further enhances the SNR (Signal-to-Noise Ratio) as well as LN Detection (LND). This improvement contributes to more accurate detection results. Overall, the optimized A- EfficientDet model shows promising performance by the sensitivity, specificity, and F1 score as shown in figure 1. This indicates its potential for clinical applications, such as early osteosarcoma detection and treatment monitoring.

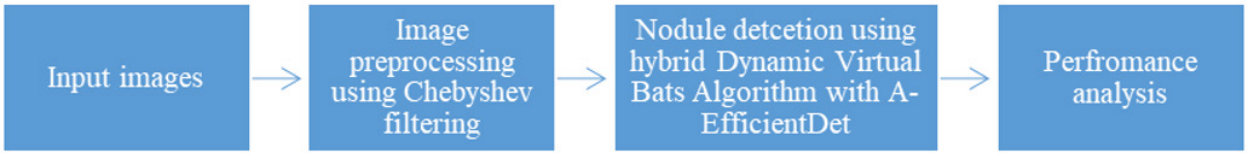

Figure 1. Smartart of proposed osteosarcoma lung nodule detection framework

The research is prearranged as follows: the related work section 2 reviews relevant literature, highlighting the uniqueness of the proposed hybrid approach. The methodology section 3 describes in detail the integration of the Dynamic Virtual Bats Algorithm (DVBA) with the Attention-based EfficientDet model, along with the inclusion of Chebyshev filtering for pre-processing. The outcomes and analysis section 4 offers the findings, comparing the optimized EfficientDet model's performance with existing methods. The conclusion summarizes the key findings and emphasizes the potential clinical applications in section 5.

Related Work

In this segment, the authors review existing literature and studies related to LND, clinical image pre-processing systems, and optimization algorithms. This provides a background for the proposed approach and highlights the novelty of the research.

For the purpose of enhancing the DE (Data Extraction) and DF (Data Fusion), a novel algorithm for the pulmonary LND was introduced by Guo et al.[15] this novel technique can be called as Multiscale Aggregation Network (MSANet). By integrating MSA algorithms, MSA effectively generates the purpose of attaining ND of different sizes, those strategies support in creating simple integration of contextual data form various resolutions. Then, FE module in the Net also enhances the interchannel and spatial data via Efficient Channel Attention and Self Calibrated Convolutions (ECA-SC). Then, it also has the potential in DE, the feature weights are modified through the extraction procedure achieved by ECA-SC.

The application of FE greatly reduces the issues via Resolution variations. This study adopted the DR (Distribution Ranking) loss as a classification LF (Loss Function), for the purpose of overcoming the imbalanced data distribution issues. CPM score of 0,920 was attained by MSANet analysis on the LUNA16 dataset. Finally, analyzing the MSANet in the PND (Pulmonary ND) demonstrated the superior outcomes in ND sensitivity thereby reducing the FP. MSANet promotes FE through effectively integrating MS data and it is considered as an advantage as it improves PND sensitivity and reducing FP. This study has some limitations, as a lack of comprehensive analysis or comparison with SOTA techniques outside of the LUNA16 dataset. It is evident that it restricts the applicability of other datasets.

For the LND, a TSCNN (Two-Stage Convolutional Neural Network) was suggested by Cao et al.[16] in the primary stage, an improved U-Net segmentation network utilizing a specific sampling technique and Two-Stage Prediction (TSP) technique were utilized. 3D-CNN classification network and a dual pooling structure for lowering the FPs were employed in the 2nd stage. A random filter was employed for generating DA (Data Augmentation) and EL (Ensemble Learning) enhances model's generalization ability. Superior detection performance was achieved by the TSCNN structure on LUNA dataset, as it was validated by the experimental outcomes.

The suggested TSCNN demonstrates competitive LND performance, validated through experiments on the LUNA dataset. One potential drawback is the limited exploration and validation of the suggested technique on diverse datasets beyond the LUNA dataset, possibly constraining its generalizability.

The Multi-Scene DL Framework (MSDLF) is necessary for an efficient LND technique, and Zhang et al.[17] suggested it, as it utilizes the vesselness filter. A 4-channel CNN architecture was developed by integrating 2

sets of images for the purpose of enhance the radiologist's ability to detect 4-stage nodules. This structure may be used in the following two modules. The results showed that the MSDLF in LND was effective in reducing FPs and enhancing accuracy over an extensive amount of image information. Across a large dataset, the suggested MSDLF provides improved accuracy and a notable decrease in FPs for LND. The lack of an extensive examination of the computational difficulty and resource needs of applying the recommended MSDLF in actual clinical settings is one possible disadvantage. According to Xi et al.[18] in real life experiments showed that PTEN amplification dramatically lowered bone degradation in OS and reduced CXCR4 levels in tumors, supporting the notion that PTEN functioned as a critical mediator between AKT and CXCR4. Moreover, treatment with the CXCR4 inhibitor AMD3100 efficiently inhibited the growth of lung and bone tumors. These results supported the use of PTEN restoration or CXCR4 blockage as possible therapies for severe OS in humans by highlighting the unique role played by the PTEN/AKT/CXCR4 signaling pathway in the progression of OS malignancy and lung metastasis. The work offers new treatment pathways by highlighting the potential treatment impact of CXCR4 inhibition or PTEN restoration in reducing lung metastasis and OS tumor growth. One drawback is the requirement for more clinical proof to verify the effectiveness and efficacy of CXCR4 inhibition or PTEN restoration as therapies for severe OS patients.

The objective of Castagnetti et al.[19] was to assess the functions of thoracotomy (TT) and thoracoscopy (TS) in pediatric patients. There were 8 thoracotomies carried out: one was a secondary procedure following an earlier TS, and the other seven were primary procedures. In 3 cases, TT revealed more nodules than CT scans; in total, TTrevealed more nodules in 7 out of sixteen cases (sensitivity, 56,2 %), mostly in cases where bilateral involvement was anticipated. In lung samples from all but 3 individuals, neoplastic tissue was discovered (86,4 %). In patients with osteosarcoma, lung nodules are usually metastases, and CT images may not always identify every lesion, particularly when bilateral involvement is anticipated. For patients with more than one thoracic nodule and excision of all metastases as the surgical goal, a thoracotomy approach may have been preferable. The study provides valuable insights into the efficacy of thoracoscopy and thoracotomy in detecting lung nodules, aiding in surgical decision-making for pediatric patients with osteosarcoma. One limitation is the retrospective study nature, potentially introducing biases and limiting the generalizability of the findings.

Utilizing image editing software, Punwani et al.[20] created a simulated nodule at the lung's periphery on an axial CT slice. Multiple copies of the altered picture were produced with different degrees of overlaid noise. The method of creating the images was carried out again for various nodule dimensions. Four Fellows of The Royal College of Radiologists independently read the output photos for a specific nodule dimensions. For the SNR ranges of 0,8–0,99, 1-1,49 %, and 1,5–2,35, the overall sensitivities and specificities for ND were 40,5 %, 77,3 %, and 90,3 %, respectively, and 47,9 %, 73,3 %, and 75 %, accordingly. As nodule dimensions and SNR grew, increasing the sensitivity for LND. At SNRs higher than 1,5, it achieved 100 % sensitivity for the nodule detection with a diameter of 4–10 mm. It was crucial to lower children's exposure to clinical radiation. This could be offset by decreased sensitivity and specificity together with a higher degree of ambiguity in the PND during chest CT exams. The study validates that increasing signal-to-noise ratio (SNR) improves sensitivity for LND on CT scans, particularly for larger nodules, aiding in diagnostic accuracy. One drawback is the potential limitation of the study's simulated setting, which may not fully replicate real-world conditions and variability in clinical practice.

The prognostic significance of the proportion of radiologically detectable to surgically deleted osteosarcoma lung nodules (SR/RD) was examined by Ahmed et al.[21]. Researchers analyzed data from 125 individuals who had metastasectomy for metastatic osteosarcoma. Individuals who had a high SR/RD ratio (>1) compared to those who had a low ratio (≤1) had significantly lower overall survival (OS) and postmetastasectomy event-free survival (EFS). Tumor necrosis and an SR/RD ratio >1 was associated with worse OS and postmetastasectomy EFS. The high SR/RD ratio served as a surrogate marker for incomplete metastatic tumor detection, highlighting its potential clinical relevance. The identification of a high SR/RD ratio as a prognostic marker offers potential for more informed treatment decisions and improved patient outcomes in metastatic osteosarcoma. The study's focus solely on osteosarcoma limits the generalizability of its findings to other types of metastatic cancers.

Utilizing Syngo CT Lung CAD, Salman et al.[22] evaluated the application of AI for adult LND. Two pediatric radiologists conducted a reference read of 3 mm axial images, identifying 109 nodules. 2 other pediatric radiologists evaluated the reference and compared the CAD outcomes at 3 mm and 1 mm slice thickness. At 1 mm, CAD detected 70 nodules having a sensitivity (Sn) of 39 % and a positive predictive value (PPV) of 62 %. At 3 mm, CAD detected 60 nodules having a Sn of 26 % and a PPV of 48 %. When smaller nodules were excluded based on algorithm conditions, the Sn increased to 68 % at 1 mm and 49 % at 3 mm, with no significant change in PPV (60 % at 1 mm and 48 % at 3 mm). According to the study's findings, adult lung CAD performed better at thinner slice thicknesses and rejected smaller nodules, but it still demonstrated poor sensitivity in pediatric patients. After less significant nodules were omitted and the slice thickness was narrower, the study showed that Syngo CT Lung CAD performed better at identifying lung nodules in adults. The study demonstrated that adult lung CAD is not very sensitive when it comes to young patients.

https://doi.org/10.56294/sctconf2024936

Summary: the multiscale aggregation network (MSANet) was presented by Guo et al. with the objective of improving information fusion and extraction across several scales for 3D lung nodule aggregation detection. MSANet integrated multiscale interaction strategies to effectively extract features while mitigating interference from resolution disparities, facilitating the integration of related data from neighborhood resolutions. Additionally, the network incorporated a feature extraction module leveraging ECA-SC to improve interchannel and spatial data, adapting feature weights during extraction to improve information extraction capabilities. Lerdsin Hospital contributed the patient's CT-scanned image dataset, which was gathered from 202 patient cases and utilized to train and validate the SSD-VGG16 framework. One advantage is that MSANet effectively integrates multiscale information and enhances feature extraction, leading to improved sensitivity in pulmonary nodule detection while reducing false positives. However, one drawback is the lack of detailed analysis or comparison with SOTA approaches beyond the LUNA16 dataset, limiting its generalizability to other datasets or real-world scenarios.

METHOD

The proposed methodology integrates various techniques to enhance the precision of osteosarcoma lung nodule detection as illustrated in figure 2. Here's a breakdown of the methodology:

- Pre-processing with Chebyshev Filtering: the methodology starts with the pre-processing of medical images, particularly CT scans for osteosarcoma lung nodule detection. Chebyshev filtering is introduced into the pre-processing pipeline. Chebyshev filtering is a technique used for signal processing and image enhancement. Its application is aimed for enhancing the quality and informativeness of the clinical images, which can lead to better detection results.
- Dynamic Virtual Bats Algorithm (DVBA): a hybrid technique with DVBA is employed. The biologically stimulated bat's nature of echolocation for stimulating the optimization procedure was performed by DBVA. Here, it serves for enhancing the framework's detection. It also enhances the efficiency and OS LND.
- Attention-based EfficientDet (A-EfficientDet): attention-based EfficientDet (A-EfficientDet) is an enhancement of the EfficientDet framework. The system's ability to identify subtle patterns suggestive of OS lung nodules can be extended by using attention appliances, which enable the structure to highlight pertinent features and suppressing those that are unnecessary.
- Hybridization of DVBA and A-EfficientDet: by combining the A-EfficientDet model and the DVBA optimization technique, the process suggests a hybrid approach. By combining the best features of both approaches, this fusion may improve the accuracy of LND. The combination of A-EfficientDet and DVBA optimization yields a hybridized framework known as the "optimized A-EfficientDet framework." When it comes to OS LND, this approach is predicted to provide greater accuracy than conventional detection techniques.
- Experimental Validation: the suggested technique was analyzed by the experiments. It's efficiency can be revealed by the outcomes of those experiments, it indicates that high accuracy rate is attained by this study. For analysing the efficiency of the suggested framework, the following measures can be employed for comparison: F1 score, sensitivity, specificity, and accuracy.

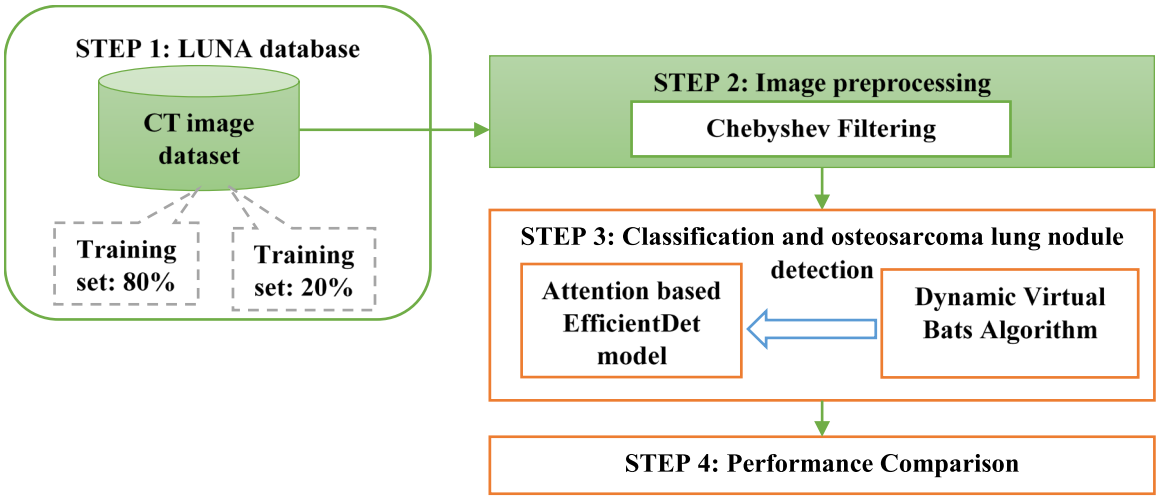

Figure 2. Architecture diagram of proposed osteosarcoma lung nodule detection model

Dataset Description

The SIEMENS SOMATOM DEFINITION 64 machines at Lerdsin Hospital in Thailand provided DICOM files from which CT-scanned PNG-like images were extracted.[23] The utilization of these images for research has been

approved by the Human Research Ethics Committee of Thammasat University (Science) (HREC-TUSc) and the RECof Lerdsin Hospital, Department of Medical Services, Ministry of Public Health in Thailand. The collection contains images from 202 individuals at Lerdsin Hospital who were diagnosed with OS. The DICOM files were transformed into CT-scanned PNG-like images for analysis when lung scans were completed. There are abnormal nodules in 2 212 of the 269 025 image files which have been obtained from the patients' DICOMs.

Image Pre-processing using Chebyshev filters

Chebyshev filters are a type of filter that is typically used in signal processing and image processing (IP) for applications including (NR) Noise Reduction.[24] They are made to achieve a sharp cutoff while reducing ripple in the passband or stopband of a filter's frequency response. Chebyshev filters can be employed to selectively filter out noise while maintaining significant image features in the framework of IP.

The general equation for a Chebyshev filter's frequency response is:

$$H(\omega) = \frac{1}{\sqrt{1+\epsilon^2 T_n^2\left(\frac{\omega}{\omega_c}\right)}} \qquad (1)$$

Here, the nth order Chebyshev polynomial can be denoted as $T_n(x)$, the ripple factor that controls the amount of ripple allowed in the passband, the angular frequency can be denoted as ω, and the cutoff angular frequency is symbolized as ω_c. Then, $H(\omega)$ is the frequency filter response. Using equation 1, one can apply a Chebyshev filter in the frequency domain to reduce noise in images. By dissecting the Chebyshev filter equations, the individual components can be examined entirely:

Chebyshev Polynomial $T_n(x)$

Chebyshev polynomials are a sequence of orthogonal polynomials that satisfy a certain recurrence relation. The nth Chebyshev polynomial is denoted as $T_n(x)$ and is defined recursively as follows

$$T_0(x) = 1,\ \ T_1(x) = x,\ T_{n+1}(x) = 2xT_n(x) - T_{n-1}(x) \qquad (2)$$

The process is described below

1. Frequency Domain Processing: in image processing, images are represented in the spatial domain (pixel intensities). On the other hand, researchers can examine and work with images according to their frequency components by transforming them into the frequency domain utilizing methods such as the Fast Fourier Transform (FFT).
2. Filtering in Frequency Domain: once the image is in the frequency domain, we can apply filtering operations directly to the frequency components. For noise reduction, we design a Chebyshev filter in the frequency domain. This involves determining the filter's parameters such as order, ripple factor, and cutoff frequency.
3. Filtering Operation: we multiply the Fourier transform of the image by the frequency response of the Chebyshev filter. This multiplication attenuates certain frequency components according to the filter's characteristics while preserving others.
4. Inverse FFT: after filtering, we convert the filtered image back to the spatial domain using the inverse FFT. This process yields the final filtered image where noise has been reduced based on the characteristics of the applied filter.

Classification and osteosarcoma lung nodule detection using an optimized A-EfficientDet model

To achieve accurate OS LND diagnosis, the suggested methodology combines the DVBA with an A-EfficientDet model and Chebyshev filtering for image enhancement. This hybrid approach improves image quality and focuses the model on relevant features. Experimental outcomes validate the efficacy of the optimized A-EfficientDet framework in achieving accurate nodule detection.

A-EfficientDet model: the Google Brain Team introduced EfficientDet, which primarily leverages 2 building blocks: the EfficientDet detector and a bidirectional feature pyramid network (BiFPN).[25] In (CV) Computer Vision, storing multilevel features has frequently been a bottleneck; one of the most frequently utilized algorithms in this regard is FPN. The unidirectional flow of data has prompted further investigation.[26] Nevertheless, these methods usually resize and sum up the features to a similar resolution, which makes their contributions to the fused result equal insufficient given their disparate resolutions. Furthermore, computing such procedures is typically prohibitively expensive. BiFPN was first presented by Nawaz et al.[27] using both top-down and bottom-up multiscale (FF) Feature Fusion. Personalized weights are learned to penalize the features based on their

https://doi.org/10.56294/sctconf2024936

relevance. 3 intuitions serve as the basis for BiFPN: 1) A node that lacks FF and only has one input edge will probably contribute less to the feature network; 2) extra edges are used to connect input and output nodes at the same level, allowing for the most cost-effective FF; and 3) all bidirectional (top-down and bottom-up) route is considered a single feature layer that is continual multiple times in order to facilitate high-level FF.

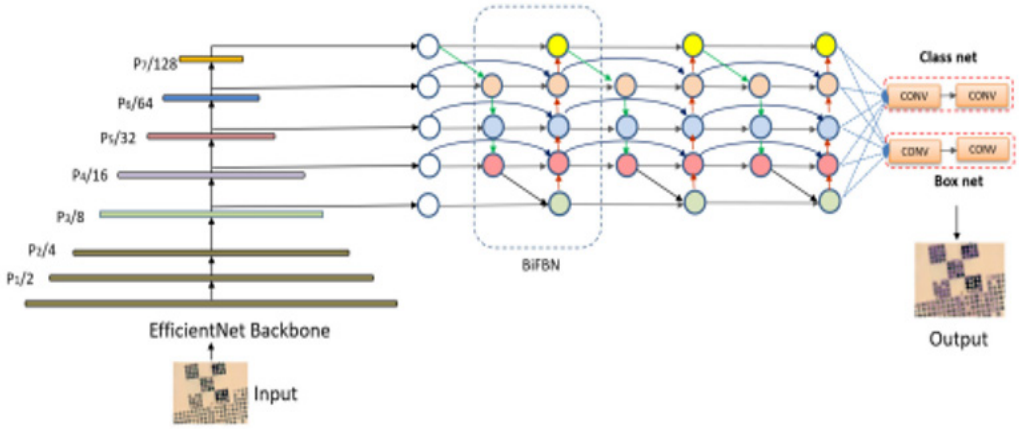

Figure 3. Architecture of EfficientDet Method[27]

There are 3 methods to calculate the weights assigned to the features. “Unbounded fusion” is the name of the initial one, and it is stated as:

$$O = \sum_i w_i . I_i \qquad (3)$$

Here, the w_i, for each feature, channel, or pixel, is a learnable weight that might be a scalar, vector, or multidimensional tensor. The fact that the scalar weight in this technique is unbounded is a drawback that could make training more difficult. In the second, a “Softmax fusion” is created as given below:

$$O = \sum_i \frac{e^{w_i}}{\sum_j e^{w_j}} . I_i \qquad (4)$$

Although this approach has a considerably larger latency cost, it ensures feature contribution preservation and bounds the weight within [0, 1]. A “fast normalized fusion” is provided in the third instance as:

$$O = \sum_i \frac{w_i}{\varepsilon + \sum_j w_j} . I_i \qquad (5)$$

Here, the input features can be denoted as I_i, ε is a tiny positive constant that is set at 0,0001 for numerical stability, and $w_i \geq 0$ is verified for each w_i using a ReLU function. Because it guarantees a bounded weight and a quicker response, this method is preferred. The EfficientDet architecture figure 2 uses a 1-stage detection approach. It is expected that EfficientDet is the basis. Then, BiFPN is implemented as a feature network, pulling features from the third through seventh tiers of the backbone. The fused output is sent to a bounding box prediction network and a class. There are strong benefits to integrating attention mechanisms into the EfficientDet framework for OS LND. First, the algorithm has the ability to identify pertinent aspects in CT images that are essential for ND since attention mechanisms allow for selective focus. By removing unnecessary data to increase detection accuracy, this selective attention also helps to NR. Furthermore, the model’s contextual understanding, which is essential for differentiating nodules among intricate anatomical structures is derived from attention mechanisms. Additionally, the interpretability provided by attention mechanisms increases confidence in the model’s predictions and makes working with medical specialists easier.

In general, the EfficientDet framework performs better in OS ND when attention mechanisms are integrated, which makes it a potential method for automated MIA (Medical Image Analysis). The following are the steps of the A-EfficientDet framework:

1. Feature Extraction: to get DE at many scales, the input image is passed over a convolutional backbone (such as EfficientNet).
2. Multi-scale Feature Fusion: in order to recognize both local and global context, features from several scales are merged. This fusion method facilitates effective handling of items of various dimensions.

https://doi.org/10.56294/sctconf2024936

3. Attention Mechanism: for the purpose of minimizing unimportant features and selectively emphasize crucial ones, attention modules are added to the basic structure of the network. These attention mechanisms can be implemented in various ways, such as using self-attention mechanisms like those found in transformers or spatial attention mechanisms like those in spatial transformer networks.

4. Prediction Heads: after the attention mechanism, prediction heads are attached to the network to output bounding box coordinates and class probabilities for detected objects.

Here's a simplified formula to illustrate how an attention mechanism might be applied within the EfficientDet architecture: let's denote the feature maps at a particular layer of the network as X_i, and A_i as the attention weights applied to these feature maps. The attended feature maps X_i^{att} can be computed as:

$$X_i^{att} = A_i \odot X_i \qquad (6)$$

Where $\odot$ denotes element-wise multiplication. The attention weights A_i can be computed based on the input feature maps X_i and some learnable parameters. For instance, in a self-attention mechanism, A_i might be computed using a softmax function applied to the pairwise similarities between the feature vectors in X_i. Table 1 shows a pseudocode representation of the EfficientDet framework incorporating the attention mechanism:

Table 1. A Pseudocode Representation of the A-efficientdet Framework

Input: input pre-processed images **Output: classified probabilities and boundary box detection**
Step 1: feature extraction • Def feature extraction (input image) • Features extraction through convolutional backbone = convolutional backbone (input image) • Return features
Step 2: multi-scale Feature Fusion • Def multi scale feature fusion(features): • Fused features = feature fusion(features) # Perform feature fusion to capture local and global context information • Return fused features
Step 3: attention Mechanism def attention mechanism(features): • Attention weights = calculate attention weights(features) # Apply attention mechanism to selectively highlight important features • Attended features = apply attention (features, attention weights) • Return attended features
Step 4: prediction heads • Def prediction heads (attended features) • Bounding box coordinates, class probabilities = prediction heads (attended features) # Attach prediction heads to output bounding box coordinates and class probabilities • Return bounding box coordinates, class probabilities
Main function to integrate all steps def A-efficientdet(input image): • Feature Extraction features = feature extraction (input image) • Multi-scale Feature Fusion fused features = multi scale feature fusion(features) • Attention Mechanism attended features = attention mechanism (fused features) • Prediction Heads bounding box coordinates, class probabilities = prediction heads (attended features) • Return bounding box coordinates, class probabilities.

DVBA method: the DVBA is a MH optimization procedure stimulated by the echolocation nature of bats. [28] It is a variant of the Bat Algorithm (BA) recommended through Xin-She Yang in 2010. DVBA extends BA by incorporating dynamic strategies to adaptively adjust its parameters during the optimization process, enhancing its exploration and exploitation capabilities. Here's a detailed explanation of the DVBA:

- Parameters Initialization: initialize the population of virtual bats with random solutions. Define parameters such as population size, frequency, loudness, pulse rate, etc.
- Objective Function: define the (OF) Objective Function to be enhanced. Here the accuracy of A-EfficientDet is fixed as objective function.

Dynamic Adaptation: dynamic Adaptation in DVBA involves the integration of mechanisms that adjust algorithm parameters, strategies, and exploration-exploitation balance dynamically throughout the optimization process.

https://doi.org/10.56294/sctconf2024936

These adaptations are based on feedback from the problem landscape and the algorithm's performance, allowing DVBA to effectively explore solution spaces, handle changing problem dynamics, and converge towards optimal or near-optimal solutions efficiently. By continuously adapting its behavior and strategies, DVBA[29] demonstrates improved robustness, versatility, and effectiveness in solving optimization problems across various domains.

Adaptive Loudness (A): the loudness (A) of the bat is adjusted dynamically during the optimization process to control the exploration and exploitation trade-off. It decreases with each iteration to reduce exploration as the algorithm progresses.

$$A_t = A_{initial} \times \alpha^t \quad (7)$$

Where A_t is the loudness at iteration t, $A_{initial}$ is the initial loudness, and α is the loudness reduction factor (usually a value between 0 and 1).

Adaptive Pulse Rate (r): the pulse rate (r) determines the frequency of bat emission. A higher pulse rate enhances the exploration capability. Similar to loudness, pulse rate is adapted dynamically:

$$r_t = r_{\min} + (r_{\max} + r_{\min}) \times \beta \quad (8)$$

Where r_t is the pulse rate at iteration t, r_{min} and r_{max} are the minimum and maximum pulse rates, and ß is a random value between 0 and 1.

Dynamic Frequency (f): the frequency (f) determines the wavelength of the emitted pulses. It is usually kept constant in traditional BA, but in DVBA, it can be adjusted to balance exploration and exploitation:

$$f_t = f_{\min} + (f_{\max} - f_{\min}) \times \gamma \quad (9)$$

Where f_t is the frequency at iteration t, f_{min} and f_{max} are the minimum and maximum frequencies, and γ is a random value between -1 and 1.

Movement of Bats: the DVBA utilizes a combination of randomized exploration and targeted search to imitate the movement of VB, which are stimulated by the echolocation behavior of real bats. The 3 primary components of a VB's behavior are its velocity, loudness, and pulse emission rate. Every VB represents a possible solution in the search space. To search their environment to identify prey (optimal solutions), bats release pulses. While loudness and pulse emission rate regulate the strength and frequency of echolocation pulses, respectively, velocity controls the distance traveled and the direction in which it moves. Bats are able to efficiently explore the solution space with the interaction of these parameters, balancing exploration to identify novel areas with exploitation to enhance solutions that are effective.

Echolocation Behavior: bats produce loud pulses and pay attention to the echoes to locate prey. In DVBA, bats represent candidate solutions, and their movements are determined by their loudness, pulse rate, and frequency.

Update Bat Position: the position of each bat is updated based on its current position, loudness, pulse rate, and frequency. The new position is determined using the following equation:

$$\mathrm{NP} = \mathrm{CP} + \mathrm{Velocity}$$
$$\mathrm{Velocity} = (\mathrm{BS} - \mathrm{CP}) \times A_t + (r_t \times r() \times (f_t \times \max range - \min range)) \quad (10)$$

Where BS is the best solution found so far, CP is current position, a random number among 0 and 1 is r(), and max range and min range define the search space.

Updating the Best Solution: compare the OF values of the current solutions with the best solution found so far. If a new solution is better than the current best solution, replace it.

Termination: terminate the algorithm when a termination condition is met (e.g., maximum amount of iterations reached, convergence achieved).

Return: return the best solution found during the optimization process.

Proposed optimized A-EfficientDet Model: for the purpose of enhancing A-EfficientDet's performance in OD tasks, its numerous parameters and configurations are optimized by the use of the DVBA in hyperparameter tuning. The general process of applying DVBA to A-EfficientDet hyperparameter adjustment is as follows:

1. Define Hyperparameters: identify the hyperparameters of A-EfficientDet that need to be optimized. Determine which hyperparameters of the attention-based EfficientDet model you want to tune. These may include learning rate, batch size, dropout rate, attention mechanism parameters, etc.
2. Define Objective Function: create an objective function that quantifies the performance of A-EfficientDet on a specific dataset and evaluation metric (e.g., accuracy). The objective function should

https://doi.org/10.56294/sctconf2024936

take the hyperparameters as input and return a value to be maximized or minimized.

3. Initialization: initialize a population of virtual bats representing different sets of hyperparameters. Randomly sample initial values for each hyperparameter within predefined ranges.

4. Evaluation: evaluate the performance of each virtual bat (set of hyperparameters) by training A-EfficientDet on a training dataset and evaluating its execution on a validation dataset using the defined objective function.

5. Update Positions: update the positions of virtual bats based on their performance. Virtual bats with better-performing hyperparameters are given higher loudness and pulse emission rates, encouraging them to explore the solution space further.

6. Dynamic Adaptation: employ dynamic adaptation mechanisms within DVBA to adjust parameters such as loudness, pulse emission rate, and velocity during the optimization process. This allows the algorithm to dynamically balance exploration and exploitation based on the problem landscape and performance feedback.

7. Termination Criterion: determine a termination criterion based on the convergence of the optimization process or a predefined number of iterations.

8. Final Model Selection: once the optimization process is complete, select the set of hyperparameters that yield the best performance on the validation dataset.

9. Evaluation on Test Set: evaluate the final selected model (A-EfficientDet with optimized hyperparameters) on an unseen test dataset to assess its generalization performance.

Table 2. Algorithm steps involved in hyperparameter tuning using dvba for a-efficientdet

Input: initialize the hyperparameters of a-efficientdet model, population of dvba and maximum iterations. Output: hyperparameters of a-efficientdet model
Step 1: define hyperparameters and objective function Hyperparameters = {'learning_rate': (0,001, 0,01), 'batch_size': (16, 64), # define other hyperparameters and their ranges • Def objective function(hyperparameters): train a-efficientdet with given hyperparameters, evaluate performance using validation dataset, return performance metric (e.g., accuracy) • Return performance metric Step 2: initialization, population size = 10, max iterations = 100 • Bats = initialize virtual bats (population size, hyperparameters) Step 3-7: dynamic virtual bats algorithm • For iteration in range (max iterations): • For bat in bats: • Update position of bat based on loudness, pulse emission rate, and velocity • Explore the solution space and evaluate performance performance = objective function(bat.hyperparameters) • Update bat's position and loudness/pulse emission rate based on performance • Update parameters of virtual bats based on dvba mechanisms • End for Step 8: final model selection • Best bat = select best bat (bats) • Best hyperparameters = best bat.hyperparameters Step 9: evaluation on test set • Final model performance = objective function (best hyperparameters) End for

A-EfficientDet's hyperparameters can be adjusted using DVBA to improve efficiency and adaptability on various OD (Object Detection) work and datasets. As indicated in table 2, the pseudocode describes the primary procedures for hyperparameter tuning with DVBA for A-EfficientDet.

It includes initialization of virtual bats with random hyperparameters, the optimization loop where bats explore the solution space and update their positions based on performance, final selection of the best-performing set of hyperparameters, and evaluation of the final model on a test dataset. Actual implementation details, such as updating mechanisms and termination criteria, may vary based on specific requirements and problem characteristics.

https://doi.org/10.56294/sctconf2024936

Figure 4. Flowchart of DVBA for hyperparameter tuning of A-Efficient model

RESULTS AND DISCUSSION

In this research, preprocessing of the CT scan images was conducted to enhance their quality for deep learning analysis. This included image normalization, illumination and contrast correction, noise reduction, and background removal. As original CT images from hospitals may contain artifacts and undesirable elements such as low-intensity levels, noise, and textual information, preprocessing steps were essential to ensure better model learning, generalization, and robustness. Additionally, specific filters like high-pass filters were applied to extract relevant information, such as clear lung images.

To validate the accuracy of ground truths, a panel consisting of 1 radiologist and 2 oncology experts independently examined the CT images for abnormal nodules detection associated with Osteosarcoma metastatic disease. Consensus was reached if at least two out of the three experts agreed on the presence of nodules. These labeled CT images were then separated into training and validation sets, comprising 80 % (1 769 images) and 20 % (443 images) of the dataset, respectively. The dataset primarily focuses on the detection of Osteosarcoma nodules, ensuring the model's training and validation on relevant pathological features. In traditional medical screening methods, accuracy is typically calculated based on the number of patients rather than individual images. If a patient has at least one correctly detected abnormality (such as a nodule), the case is considered positive. However, in engineering-oriented approaches like the one described in this section, a different method is employed to provide deeper analysis focusing on both quantity and quality.

Instead of aggregating results at the patient level, the engineering standard method evaluates accuracy based on the number of images. This proposed optimized A-EfficientDet approach allows for a more detailed analysis of each individual image, considering every detail in the dataset. While using the number of images to calculate accuracy may result in a lower overall accuracy compared to patient-level aggregation, it provides insights into the execution of the procedure on a per-image basis. By adopting the number of image approach, the evaluation can capture finer details and nuances in the detection process, which may be missed when considering only patient-level outcomes. This approach enables a more granular assessment of the algorithm's performance, facilitating improvements in both detection quantity and quality across the entire dataset.

https://doi.org/10.56294/sctconf2024936

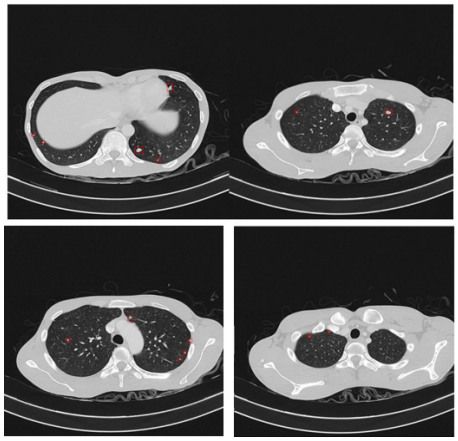

Figure 5. Example of the labelled CT-Scanned nodule images

The proposed optimized A-EfficientDet is compared with exiting methods such as MSANet[15], TSCNN[16] and SSD-VGG16[23] depends on performance matrix such as precision, recall, f-measure and accuracy. In the evaluation process, a corrected predicted nodule is considered a True Positive (TP) outcome. To compute performance scores, the True Negative (TN) value must also be obtained. Since the evaluated images did not originally contain non-nodule CT-scanned images, these non-nodule images were added to the evaluation set to obtain the False Positive (FP) value. These non-nodule CT-scanned images are referred to as "no-class" images. Given the absence of a typical technique for adding no-class images, one non-nodule image was employed in this study as one object in the image. The amount of TP discovered from the first evaluation of the photos was equal to the number of non-nodule photographs added during the review procedure. The common performance scores used in this evaluation are the F1-score and accuracy. The F1-score is calculated using the harmonic mean of Precision and Recall, which are calculated as follows:

$$Recall = \frac{TP}{TP+FN} \quad (10)$$

$$Precision = \frac{TP}{TP+FP} \quad (11)$$

The F1-score is then calculated as:

$$F1 - score = 2 \times \frac{Precison \times recall}{Precison+recall} \quad (12)$$

Additionally, accuracy is calculated using the formula:

$$accuracy(\%) = \frac{TP+TN}{TP+FP+TN+FN} \times 100\% \quad (13)$$

These performance metrics provide an inclusive assessment of the procedure's detection performance, considering both the precision and recall of nodule detection as well as the total accuracy of the framework.

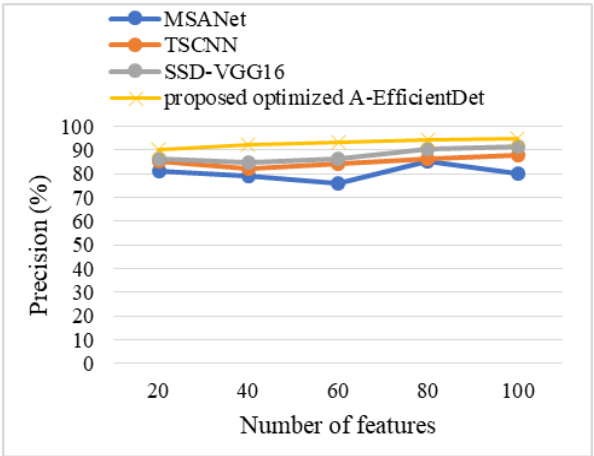

Figure 6. Precision performance comparison

https://doi.org/10.56294/sctconf2024936

Figure 6 presents the outcomes of a precision comparison among the recommended optimized A-EfficientDet and the traditional MSANet, TSCNN, and SSD-VGG16 classifiers. The table indicates that the suggested approach provides a high rate of accuracy when compared to other current methods. It is a very successful method with a 95 % accuracy rate in attack detection. MSANet, TSCNN, and SSD-VGG16 provide noteworthy accuracy rates of 80 %, 88,5 %, and 91,5 %, respectively, when analyzing the accuracy of current approaches. Effective preprocessing, such as contrast correction and NR, improves image clarity and is responsible for the high precision reached by the recommended approach. The accuracy with which various specialists identify nodules and the methodical management of FPs also add to the reliability of ND.

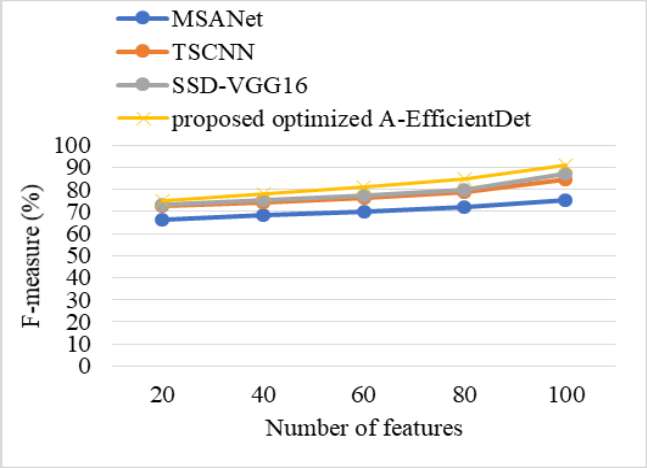

Figure 7. F-measure performance comparison

The F-measure comparison outcomes for the SSD-VGG16, MSANet, TSCNN, and suggested enhanced A-EfficientDet classifiers are presented in figure 7 According to the statistics, the suggested enhanced A-EfficientDet has an exceptionally high F-measure rate of 91 %. Among the existing approaches, MSANet, TSCNN, and SSD-VGG16 give lower rates of 73,15 %, 84,5 %, and 87 %, respectively, in comparison to the rate of the F-measure. This suggests that the suggested approach can outperform the earlier solutions in terms of attack detection results. Effective ND while reducing FPs and FNs is made possible by the balanced optimization of precision and recall, which is made possible by reliable OD algorithms and accurate ground truth labeling. This leads to the high F-measure.

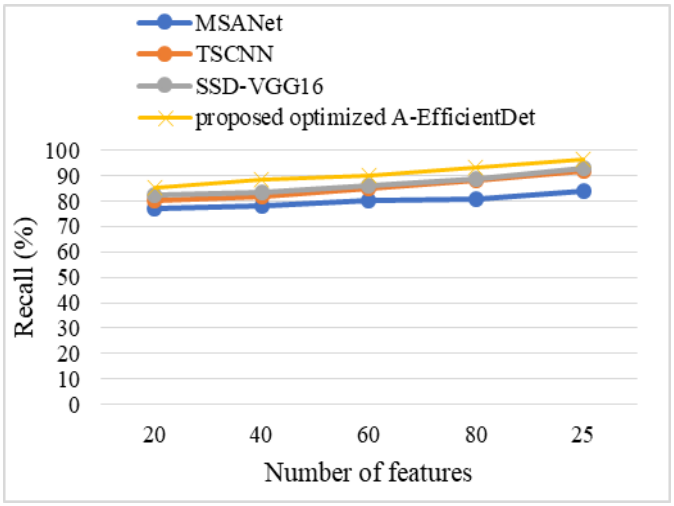

Figure 8. Recall performance comparison

Figure 8 displays the recall comparison outcomes for the SSD-VGG16, TSCNN, MSANet, and recommended optimized A-EfficientDet classifiers. The 96 % recall rate offered by the suggested method is incredibly high. These results indicate that the optimized A-EfficientDet that has been recommended has a high memory rate and an average attack detection rate. It is evident from comparing the recall rates of the existing techniques that the suggested system can outperform the older techniques in terms of attack detection results. Recall rates for MSANet, TSCNN, and SSD-VGG16 are 84 %, 92 %, and 93 %, respectively. Extensive coverage of nodule

https://doi.org/10.56294/sctconf2024936

variation is ensured by using sophisticated OD networks trained on a variety of datasets, in conjunction with careful preprocessing to improve image quality to achieve high recall. Furthermore, complete ND across CT scan images is ensured by the improved A-EfficientDet-based labeling approach by various experts, which eliminates FNs and manages FPs in an organized manner.

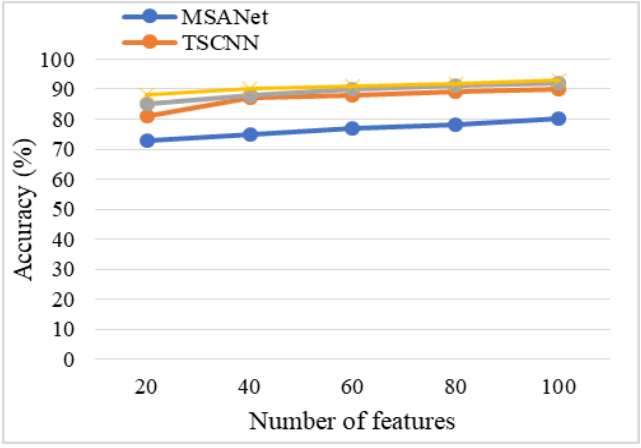

Figure 9. Accuracy performance comparison

The attack detection accuracy comparison can be observed in the graph in figure 9 above. Techniques like optimized A-EfficientDet multiclass classifiers, TSCNN, Optimized AE+DNN, and MSANet are applied. The optimized A-EfficientDet has a high accuracy rate of 93 %, making it a great way to get precise predictions. The accuracy rates of previous techniques such as MSANet, TSCNN, and SSD-VGG16 are 80 %, 90 %, and 92 %, respectively. The improved A-EfficientDet algorithms for learning allow for higher accuracy while addressing the local optima problem since the results are more susceptible to noise in the training set. The suggested methodology achieves high accuracy through rigorous preprocessing techniques that enhance image quality, coupled with the utilization of advanced object detection networks trained on diverse datasets. Also, meticulous monitoring of FPs and precise ground truth labeling by several specialists enhance the reliability of ND, leading to improved efficiency.

CONCLUSIONS

In conclusion, a potential method for accurateLND of osteosarcoma is the hybrid DVBA with Attention-based Efficient OD(A-EfficientDet). Significant gains in detection performance and accuracy are made by optimizing the A-EfficientDet model using the DVBA optimization technique and adding Chebyshev filtering into the pre-processing process. The outcomes of the experiment show remarkable results: 93 % accuracy, 96 % recall, 91 % F-measure, and 95 % precision in LND from OS. These results highlight how well the suggested approach enhances MIA and makes it easier to identify significant disorders earlier. Future research and development of the suggested hybrid strategy might concentrate on the following domains:

- Enhanced Preprocessing Techniques: investigating additional preprocessing methods and techniques to further improve image quality and enhance FE, potentially leading to even higher detection accuracy rates.
- Algorithm Optimization: continuously optimizing and fine-tuning the other recent novel hybrid deep learning model to improve its efficiency, robustness, and adaptability across different MI datasets and modalities.
- Integration of Multi-Modal Data: exploring the integration of multi-modal MI data, such as combining CT scans with MRI or PET scans, to deliver a more inclusive and accurate prediction and classification of OS and other pulmonary pathologies.

By addressing these avenues for future research, the proposed methodology can further advance the field of medical imaging analysis, ultimately improving patient outcomes and facilitating more effective clinical decision-making.

BIBLIOGRAPHIC REFERENCES

1. Kager L, Tamamyan G, and Bielack S. Novel insights and therapeutic interventions for pediatric osteosarcoma. Future Oncology, 13(4), pp. 357-368. https://doi.org/10.2217/fon-2016-0261.

2. Aljubran AH, Griffin A, Pintilie M, and Blackstein M. Osteosarcoma in adolescents and adults: survival analysis with and without lung metastases. Annals of Oncology, 20(6), pp. 1136-1141. https://doi.org/10.1093/annonc/mdn731.

3. Kager L, Zoubek A, Pötschger U, Kastner U, Flege S, Kempf-Bielack B, Branscheid D, Kotz R, Salzer-Kuntschik M, Winkelmann W, and Jundt G. Primary metastatic osteosarcoma: presentation and outcome of patients treated on neoadjuvant Cooperative Osteosarcoma Study Group protocols. Journal of clinical oncology, 21(10), pp. 2011-2018. https://doi.org/10.1200/JCO.2003.08.132.

4. Cao K, Xu J, and Zhao WQ. Artificial intelligence on diabetic retinopathy diagnosis: an automatic classification method based on grey level co-occurrence matrix and naive Bayesian model. International journal of ophthalmology, 12(7), pp. 1158–1162. https://doi.org/10.18240%2Fijo.2019.07.17.

5. Choi WJ, and Choi TS. Automated pulmonary nodule detection based on three-dimensional shape-based feature descriptor. Computer methods and programs in biomedicine, 113(1), pp. 37-54. https://doi.org/10.1016/j.cmpb.2013.08.015.

6. Peña DM, Luo S, and Abdelgader AM. Auto diagnostics of lung nodules using minimal characteristics extraction technique. Diagnostics, 6(1), p. 1-14. https://doi.org/10.3390/diagnostics6010013.

7. Camarlinghi N, Gori I, Retico A, Bellotti R, Bosco P, Cerello P, Gargano G, Lopez Torres E, Megna R, Peccarisi M, and Fantacci ME. Combination of computer-aided detection algorithms for automatic lung nodule identification. International journal of computer assisted radiology and surgery, 7, pp. 455-464. https://doi.org/10.1007/s11548-011-0637-6.

8. Teramoto A, and Fujita H. Fast lung nodule detection in chest CT images using cylindrical nodule-enhancement filter. International journal of computer assisted radiology and surgery, 8, pp. 193-205. https://doi.org/10.1007/s11548-012-0767-5.

9. Thomas RA, and Kumar SS. Automatic detection of lung nodules using classifiers. In International Conference on Control, Instrumentation, Communication and Computational Technologies (ICCICCT), pp. 705-710. https://doi.org/10.1109/ICCICCT.2014.6993051.

10. Santos AM, de Carvalho Filho AO, Silva AC, De Paiva AC, Nunes RA, and Gattass M. Automatic detection of small lung nodules in 3D CT data using Gaussian mixture models, Tsallis entropy and SVM. Engineering applications of artificial intelligence, 36, pp. 27-39. https://doi.org/10.1016/j.engappai.2014.07.007.

11. Wang K, Shou Q, Ma SJ, Liebeskind D, Qiao XJ, Saver J, Salamon N, Kim H, Yu Y, Xie Y, and Zaharchuk G. Deep learning detection of penumbral tissue on arterial spin labeling in stroke. Stroke, 51(2), pp. 489-497. https://doi.org/10.1161/STROKEAHA.119.027457.

12. Wolterink JM, van Hamersvelt RW, Viergever MA, Leiner T, and Išgum I. Coronary artery centerline extraction in cardiac CT angiography using a CNN-based orientation classifier. Medical image analysis, 51, pp. 46-60. https://doi.org/10.1016/j.media.2018.10.005.

13. Ni YL, Zheng XC, Shi XJ, Xu YF, and Li H. Deep convolutional neural network based on CT images of pulmonary nodules in the lungs of adolescent and young adult patients with osteosarcoma. Oncology Letters, 26(2), pp. 1-8. https://doi.org/10.3892/ol.2023.13930.

14. Loraksa C, Mongkolsomlit S, Nimsuk N, Uscharapong M, and Kiatisevi P. Effectiveness of learning systems from common image file types to detect osteosarcoma based on convolutional neural networks (CNNs) models. Journal of Imaging, 8(1), p. 1-20.

15. Guo Z, Zhao L, Yuan J, and Yu H. Msanet: multiscale aggregation network integrating spatial and channel information for lung nodule detection. IEEE Journal of Biomedical and Health Informatics, 26(6), pp. 2547-2558.

16. Cao H, Liu H, Song E, Ma G, Xu X, Jin R, Liu T, and Hung CC. A two-stage convolutional neural networks for lung nodule detection. IEEE journal of biomedical and health informatics, 24(7), pp.2006-2015. https://doi.org/10.1109/JBHI.2019.2963720.

17. Zhang Q, and Kong X. Design of automatic lung nodule detection system based on multi-scene deep learning framework. IEEE Access, 8, pp. 90380-90389. https://doi.org/10.1109/ACCESS.2020.2993872.

18. Xi Y, Qi Z, Ma J, and Chen Y. PTEN loss activates a functional AKT/CXCR4 signaling axis to potentiate tumor growth and lung metastasis in human osteosarcoma cells. Clinical & experimental metastasis, 37, pp. 173-185. https://doi.org/10.1007/s10585-019-09998-7.

19. Castagnetti M, Delarue A, and Gentet JC. Optimizing the surgical management of lung nodules in children with osteosarcoma: thoracoscopy for biopsies, thoracotomy for resections. Surgical Endoscopy And Other Interventional Techniques, 18, pp. 1668-1671. https://doi.org/10.1007/BF02637141.

20. Punwani S, Zhang J, Davies W, Greenhalgh R, and Humphries P. Paediatric CT: the effects of increasing image noise on pulmonary nodule detection. Pediatric radiology, 38, pp. 192-201. https://doi.org/10.1007/s00247-007-0694-8.

21. Ahmed G, Elshafiey M, Romeih M, Elgammal A, Kamel A, Salama A, and Zaky I. Prognostic significance of the ratio of surgically resected to radiologically detected lung nodules in patients with metastatic osteosarcoma. Surgical Oncology, 40, pp. 101701. https://doi.org/10.1016/j.suronc.2021.101701.

22. Salman R, Nguyen HN, Sher AC, Hallam KA, Seghers VJ, and Sammer MB. Diagnostic performance of artificial intelligence for pediatric pulmonary nodule detection in computed tomography of the chest. Clinical Imaging, 101, pp. 50-55. https://doi.org/10.1016/j.clinimag.2023.05.019.

23. Loraksa C, Mongkolsomlit S, Nimsuk N, Uscharapong M, and Kiatisevi P. Development of the osteosarcoma lung nodules detection model based on SSD-VGG16 and competency comparing with traditional method. IEEE Access, 10, pp. 65496-65506. https://doi.org/10.1109/ACCESS.2022.3183604.

24. Bolourchi P, Demirel H, and Uysal S. Target recognition in SAR images using radial Chebyshev moments. Signal, Image and Video Processing, 11, pp. 1033-1040. https://doi.org/10.1007/s11760-017-1054-2 .

25. Tan M, Pang R, and Le QV. Efficientdet: Scalable and efficient object detection. In Proceedings of the IEEE/CVF conference on computer vision and pattern recognition, pp. 10781-10790.

26. Mekhalfi ML, Nicolò C, Bazi Y, Al Rahhal MM, Alsharif NA, and Al Maghayreh E. Contrasting YOLOv5, transformer, and EfficientDet detectors for crop circle detection in desert. IEEE Geoscience and Remote Sensing Letters, 19, pp. 1-5. https://doi.org/10.1109/LGRS.2021.3085139.

27. Nawaz M, Nazir T, Baili J, Khan MA, Kim YJ, and Cha JH. Cxray-effdet: chest disease detection and classification from x-ray images using the efficientdet model. Diagnostics, 13(2), pp. 1-22. https://doi.org/10.3390/diagnostics13020248.

28. Topal AO, and Altun O. A novel meta-heuristic algorithm: dynamic virtual bats algorithm. Information Sciences, 354, pp. 222-235. https://doi.org/10.1016/j.ins.2016.03.025.

29. Topal AO, Yildiz YE, and Ozkul M. Dynamic virtual bats algorithm with probabilistic selection restart technique. In Transactions on Engineering Technologies: World Congress on Engineering and Computer Science, pp. 111-126. https://doi.org/10.1007/978-981-13-2191-7_9.

FINANCING

"The authors did not receive financing for the development of this research".

CONFLICT OF INTEREST

"The authors declare that there is no conflict of interest".

AUTHORSHIP CONTRIBUTION

Conceptualization: Nandhini. A.
Data curation: Sengaliappan. M.
Formal analysis: Sengaliappan. M.
Research: Nandhini. A.
Methodology: Nandhini. A.
Drafting - original draft: Sengaliappan. M.
Writing - proofreading and editing: Nandhini. A.